

## NON-ISOTHERMAL CRYSTALLIZATION IN AMORPHOUS SELENIUM FILMS

J. GRENET, J. P. LARMAGNAC and P. MICHON

*Laboratoire d'Etudes des Couches Minces Amorphes et Polycristallines, Faculté des Sciences de Rouen, F 76130 Mont-Saint-Aignan, France*

(Received July 8, 1981; in revised form March 15, 1982)

The usual determination of kinetic parameters of crystallization of amorphous products is based on isothermal measurements. In general the crystallization of amorphous selenium thin films is studied by non-isothermal experiments (DTA). The adaptation to non-isothermal crystallization of the Avrami transformation rate equation allows us to determine different types of crystallization. These different regions enable one to determine the variations of the growth rate and of the nucleation rate versus temperature. The influence of the wavelength of illumination during the crystallization time on these parameters is also investigated.

The last decades have seen a strong theoretical and experimental interest in the non-isothermal analysis techniques for the study of phase transformations. These non-isothermal techniques have several advantages: rapidity of experiment and facilities to extend the temperature range beyond that accessible to isothermal experiments. Also, many phase transformations depend on non-isothermal kinetics:

Thus it is not surprising for the study of systems in which the temperature of the interface (amorphous-crystal for example) is well defined by the temperature of the system (i.e. the difference of temperature between the interface and the system is negligible), to see differential thermal analysis (DTA) and differential scanning calorimetry (DSC) as techniques which are applicable, in particular to the study of crystallization kinetics.

### **Isothermal crystallization**

#### *Avrami equation*

The crystallized fraction  $x$  of the system at time  $t$ , is defined as follows:

$$x(t) = \frac{V_c(t)}{V_0} = 1 - \exp\left(-\frac{V_e(t)}{V_0}\right). \quad (1)$$

The volume  $V_0$  is the total volume of the sample and  $V_e(t)$  is the "extended crystallized volume", i.e. the volume which includes all the crystalline regions, assumed to be independent without taking into account possible overlapping,  $V_c(t)$  is the real crystallized volume at time  $t$ . This notion of "extended crystallized volume"

introduced by Avrami [1-3] allows one to take into account the situations where nucleation and growth occur.

We can calculate  $V_e(t)$  in the following way: if  $N$  is the nucleation rate per unit volume, at time  $t$  the volume of all crystallized regions apparently nucleated between  $t = \tau$  and  $t = \tau + d\tau$  is

$$dv_\tau = \eta Y_1 Y_2 Y_3 V_0 N(\tau) (t - \tau)^3 d\tau \quad (2)$$

where  $\eta$  is a shape factor and  $Y_i$  the growth rate in  $i$  direction. Then, in a homogeneous nucleation throughout all the sample

$$V_e(t) = \eta Y_1 Y_2 Y_3 V_0 \int_0^t N(\tau) (t - \tau)^3 d\tau \quad (3)$$

in particular for constant  $N(\tau)$

$$x(t) = 1 - \exp(-\eta Y_1 Y_2 Y_3 N t^4/4). \quad (4)$$

More generally, we have to suppose that the initial concentration of nuclei is  $N_0$  and that, in addition, the nucleation rate is represented by the law  $N(t) = C t^q$

The crystallized fraction at time  $t$  becomes

$$x(t) = 1 - \exp\{-\eta Y_1 Y_2 Y_3 (N_0 t^3 + C' t^{4+q})\}. \quad (5)$$

To take into account intermediate cases, Avrami suggests that  $x(t)$  be represented by:

$$x(t) = 1 - \exp\{-K t^n\}. \quad (6)$$

This equation is known as the Johnson-Mehl-Avrami transformation equation. In this equation  $K$  is a function of temperature and usually depends on both the growth rate and the nucleation rate,  $n$  is a parameter which reflects the nucleation rate, or the growth morphology or both.

First developed for three dimensional growth this equation was modified when sheet or wire transformation takes place.

Because of the simplicity of the Eq. (6), we shall use (6) in the developments of p. 543 relative to different ways of non-isothermal crystallization.

However, in order to determine the crystallization parameters (growth rate, nucleation rate) from the different values of  $n$  given by non-isothermal studies, we have to specify the different possible types of crystallization.

#### *Different types of crystallization*

We have to consider two types of crystallization

- bulk crystallization
- crystallization from the surface

and we have to distinguish two types of nucleation

- homogeneous nucleation
- heterogeneous nucleation (due to initial crystallites)

Moreover, it is necessary (in our case) to take into consideration the minute thickness  $e$  of the sample (thin film).

Following Germain et al [4, 5], the extended crystallized volume  $V_e(t)$  is calculated in the general situation where a crystallization occurs through homogeneous nucleation and isotropic growth. The crystallites can grow in a three dimensional way as long as their diameter is smaller than the thickness of the sample; then they grow two-dimensionally.

*Bulk crystallization*

The crystallized volume  $V_e(t)$  can be decomposed into two parts:

- $V_e^1(t)$  due to homogeneous nucleation (crystallites are created during the whole annealing period).
- $V_e^2(t)$  due to heterogeneous nucleation (crystallites existing before the annealing, with a mean radius  $a_0$ ).

Let  $S$  be the sample surface,  $v$  the growth rate,  $N$  the nucleation rate per unit volume,  $p$  the number of crystallites present at  $t = 0$  per unit surface and  $\tau$  the time necessary for a crystallite diameter to reach the thickness of the film ( $v\tau = e$ ).

Then

$$V_e^1(t) = \frac{\pi}{3} Se^2 N v^2 (t^3 - \tau^3) + \frac{\pi}{3} Se N v^3 \tau^4 \quad (t > \tau). \tag{7a}$$

and

$$V_e^1(t) = \frac{\pi}{3} Se N v^3 t^4 \quad (t < \tau) \tag{7b}$$

The value of  $V_e^2(t)$  depends on relative values of  $N$ ,  $p$ ,  $a_0$ ,  $t$  and  $\tau$ .

$$V_e^2(t) \simeq p\pi v^2 t^2 \cdot Se \quad vt \gg a_0, a_0 \geq e, p \leq \frac{1}{e^2} \tag{8a}$$

$$V_e^2(t) \simeq \frac{4}{3} p\pi (a_0 + vt)^3 S \quad t < \tau, a_0 \ll e, p \geq \frac{1}{e^2} \tag{8b}$$

$$V_e^2(t) \simeq p\pi (a_0 + vt)^2 Se \quad t < \tau, a_0 \geq e, p > \frac{1}{e^2} \tag{8c}$$

and

$$V_e(t) = V_e^1(t) + V_e^2(t)$$

$$x(t) = 1 - \exp\left(-\frac{V_e(t)}{V_0}\right)$$

$$\ln \left( \frac{1}{1-x} \right) \text{ is usually used.}$$

$$\ln \left( \frac{1}{1-x} \right) = \frac{V_e(t)}{V_0} = \frac{V_e(t)}{Se}. \quad (9)$$

See table 1 p. 6988 by Germain et al [4].

### *Crystallization from the surface*

When crystallization is induced by  $p$  cylindrical crystallites of mean radius  $a_0$  having a thickness negligible compared to the thickness  $e$  of the film and situated on the surface, we get

$$\ln \left( \frac{1}{1-x} \right) = \frac{p\pi}{e} a_0^2 vt \quad t < \tau \quad (10a)$$

and

$$\ln \left( \frac{1}{1-x} \right) = p\pi (a_0 + vt)^2 t > \tau \quad (10b)$$

These expressions suppose that the radius of the crystallites is very large compared to the thickness  $e$ . In the case  $a_0 \simeq e$ , expression (10a) is replaced by

$$\ln \left( \frac{1}{1-x} \right) = \frac{p}{e} \left( a_0^2 vt + \frac{2}{3} v^3 t^3 \right). \quad (10c)$$

### *Conclusion*

The two types of crystallization (bulk and surface) can overlap. In all cases we have an expression

$$\ln \left( \frac{1}{1-x} \right) = \lambda_1 t + \lambda_2 t^2 + \lambda_3 t^3 + \lambda_4 t^4. \quad (11)$$

The importance of each term depends on the relative influence of the different parameters of crystallization and on the elapsed time.

The Eq. (11) is similar to Eq. (6)

$$\ln \left( \frac{1}{1-x} \right) = K t^n. \quad (12)$$

In any case the regime is modified when  $t$  is equal to  $\tau$  and a determination of this change gives a measurement of  $\tau$  and consequently of  $v$ ;

The values of the parameter  $n$  allows the preponderant types of crystallization and nucleation to be determined.

### Non-isothermal crystallization – Methodology

In order to determine the changes in the regimes of the crystallization and subsequently the different parameters, we shall use differential thermal analysis. To use the Avrami equation in DTA or DSC measurements, there are several problems, mainly because this equation is an isothermal equation. As Henderson [6] points out, the Avrami equation with its restrictive assumptions (isothermal conditions, random nucleation and growth rate depending only on temperature) can be used in non-isothermal transformations only if the transformation rate depends on the state variables of the transformed fraction and of the temperature and not on the thermal history of the sample. Under these conditions, an example of a system which allows a non-isothermal application of equation (6) is the one in which the nucleation process takes place early in the transformation and the nucleation rate is null thereafter. This case is outlined as site saturation by Cahn [7, 8].

However it is possible to use Eq. (6) as an approximation in the cases in which these hypothesis are not fulfilled.

#### *Application of DTA and DSC to the measurements of crystallization kinetics*

The usual experimental imposed condition is that the temperature is changed at a constant rate  $r$ . For sufficiently small samples (low mass), a good thermal contact (in order to assure uniformity of the temperature) and for small values of  $r$  the thermal behavior of the samples can be used to determine the transformation kinetics. Figure 1 shows a typical DTA or DSC curve.

In stirred solutions, following Borchardt and Daniels [9, 10], we have:

$$\frac{dx}{dt} = \frac{C_p}{\delta H} \frac{d(\Delta T)}{dt} + \eta \Delta T \quad (13)$$

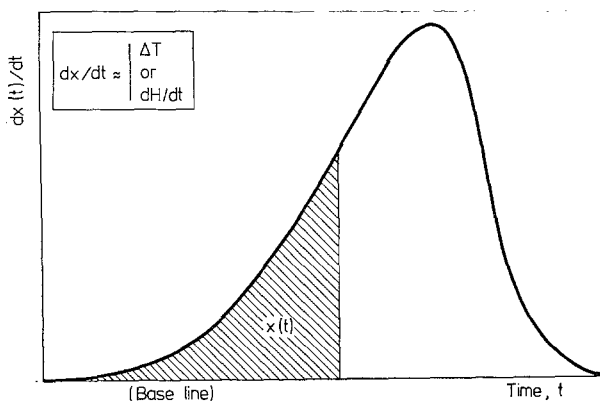


Fig. 1. Schematic drawing of DTA or DSC trace

where  $\delta H$  is the enthalpy of the transformation,  $x$  the transformed fraction of material and  $\Delta T$  the DTA signal. For a uniform temperature, we can extend this equation to solid systems, and if  $C_p/\delta H$  is very small, we can assume the ordinate of the curve  $\Delta T$  to be proportional to  $dx/dt$ . In DSC the heat evolved is proportional to the transformed fraction of material and consequently  $dx/dt \sim dH/dt$ . Thus, the area under the curve, from time  $t = 0$  to  $t$  is proportional to  $x(t)$ . We can determine the constant of proportionality by using the normalization condition:

$$\int_0^{\infty} \left( \frac{dx}{dt} \right) dt = 1.$$

From Eq. (6) we can calculate  $dx/dt$

$$\frac{dx}{dt} = nK^{1/n} (1-x) \left[ \ln \left( \frac{1}{1-x} \right) \right]^{\frac{n-1}{n}}. \quad (14)$$

This equation is known as Johnson–Mehl–Avrami transformation rate equation.

Two equations are generally chosen for  $K$

$$K = K_0 \exp(-\Delta H/kT) \quad (\text{Arrhenius law})$$

or

$$K = K_0 \exp[-\Delta H/k(T - T_0)] \quad (\text{Vogel–Fulcher law})$$

where  $\Delta H$  is an apparent activation energy,  $T_0$  a constant temperature and  $K_0$  is an appropriate preexponential term. In this paragraph  $K_0$  will be constant with respect to temperature; it is not strictly true, but as a first approximation, we can ignore the temperature dependence of  $K_0$  compared with the exponential term.

#### *Determination of $\Delta H$ and $n$ using a single scan technique*

By substituting  $\theta$  for  $T$  (Arrhenius law) or  $T - T_0$  (Vogel–Fulcher law), we can develop the Avrami equation in the same way.

#### *Determination of $\Delta H/n$*

Using the method described previously by Piloyan [11], it is possible to show that a plot of  $\ln(dx/dt)$  versus  $1/\theta$  will closely approximate to a straight line with a slope equal to  $-\Delta H/nk$  (see appendix A2).

#### *Determination of $\Delta H$ and $n$*

The plot of  $\ln(\ln(1-x)^{-1})$  versus  $\theta^{-1}$  will approximate to linear behavior with a slope equal to  $-\Delta H/k$  (see appendix A3). Both the values of  $\Delta H/n$  and  $\Delta H$  allow the determination of  $n$ .

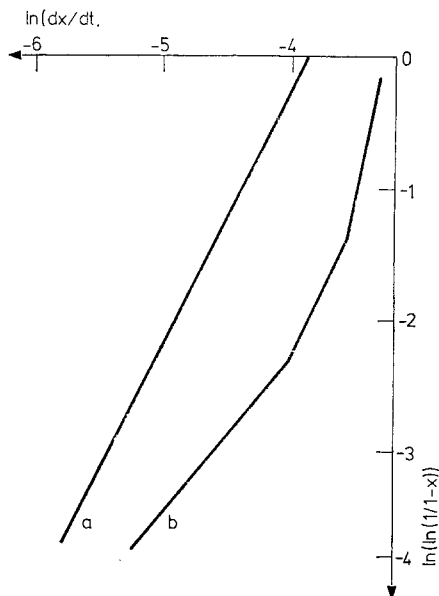


Fig. 2. Schematic curves in "reduced coordinates" a)  $n$  constant; b)  $n$  variable

But a direct plot of  $\ln(\ln(1-x)^{-1})$  vs.  $\ln(dx/dt)$  will closely approximate to a straight line with a slope equal to  $n$  (see Fig. 2). Notice that it is possible to determine  $T_0$  [6] in the case corresponding to the Vogel–Fulcher law (in this case, the plot of  $\ln(dx/dt)$  vs.  $T^{-1}$  exhibits some curvature).

#### *Multiple scan technique*

Let be  $\theta_0$  the temperature at which a fraction  $x_0$  is transformed at heating rate  $r$ . Thus, by varying the rate in a series of scans and integrating the  $dx/dt$  curves, different values of  $\theta_0$  will be obtained. A plot of  $\ln(r/\theta_0^2)$  versus  $\theta_0^{-1}$  will have a slope equal to  $-\Delta H/nk$ . This method, somewhat long, can be accelerated and simplified, if we notice [6] that, at the maximum of the peak, the fraction  $x_p$  is nearly independent on the heating rate  $r$ . The subscript index  $p$  means that the values are measured at the maximum of the transformation peak. In the peak method, the curve  $\ln(r/\theta_p^2)$  versus  $\theta_p^{-1}$  is drawn (without integration) and had a slope given by  $-\Delta H/nk$ . This method allows a quick determination of  $\Delta H/n$  and can be compared to the method of analysis outlined by Kissinger [12].

But if one does not know the value of the parameter  $n$ , discrepancies are to be formed in the interpretation of the physical meaning of  $\Delta H/n$ .

#### *n variable*

The techniques developed in previous paragraphs assume, as in Eq. (14), that  $n$  is constant during the transformation.

A similar development can be conducted with the assumption that  $n$  is variable (see appendix A4). Then a plot of  $\ln(\ln(1-x)^{-1})$  vs.  $\ln(dx/dt)$  shows several linear parts with slopes equal to the different values of  $n$  and consequently indicates the different possible regimes of crystallization. An example, in this system of coordinates we call "reduced coordinates", is shown on Fig. 2.

## Experimental results — Application to amorphous selenium

### *Sample preparation*

Aluminium substrates (6.5 mm diameter, 15  $\mu\text{m}$  thick) were placed on a substrate holder at 20 cm from the evaporation crucible. This configuration enabled us to obtain one hundred similar samples at each evaporation of a charge of 99.999% purity selenium. During the evaporation process (at a pressure of  $5 \times 10^{-7}$  torr) the substrate temperature was held at 300 K.

This temperature was 20 K below the glass transition temperature and allowed the homogeneous nucleation to be neglected during the formation of the samples [13]. The thickness of the films was about 5  $\mu\text{m}$  and their mass was 0.7 mg.

The shape of the samples allowed the conditions of page 541 to be satisfied.

### *Analysis procedure*

Analyses were conducted using a Stone differential thermal analysis system. Heating rates varied from 1 degree  $\text{min}^{-1}$  to 40 degree  $\text{min}^{-1}$  in the temperature range 273 K–433 K. The thermocouples (iron-constantan) held the aluminium disc coated by selenium and the reference aluminium disc. Directly coating aluminium with selenium permitted a better detection of thermal exchanges. The sensitivity per cm was 2.25  $\mu\text{V}$  in  $\Delta T$  scale ( $\sim 40$  mK) and 2.7 mV in the temperature scale. The fusion of a suitable mass of indium (99.99% of purity), placed on the reference disc, was used as a temperature reference.

### *Experimental conditions*

Figure 3a shows typical DTA curves obtained at various heating rates for a sample aged for one week. We observe the well known shift of the crystallization peak to the higher temperatures with increasing heating rates. This property yields crystallization processes at different temperatures. However, it is quite important not to hide this phenomenon by the shift to the lower temperatures of the crystallization peak with the age of the samples (fig. 3b) [14].

For this reason, the samples are prepared simultaneously, ageing all together at the same temperature (294 K, i.e.  $\sim 25$  K below the glass transition temperature) during the same time (4 months). This period is a sufficient time for the experimental one to be neglected compared with the ageing period).



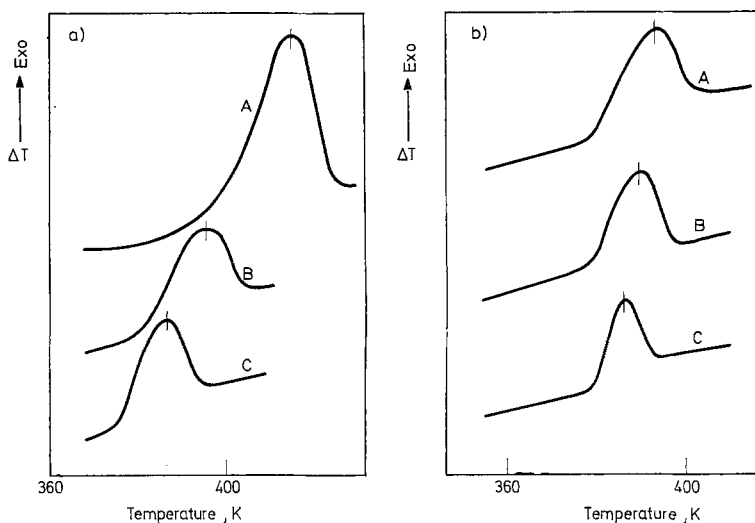


Fig. 3. Peaks of crystallization displacement. a) versus heating rate A:  $0.15 \text{ degree} \cdot \text{s}^{-1}$ ; B:  $0.05 \text{ degree} \cdot \text{s}^{-1}$ ; C:  $0.02 \text{ degree} \cdot \text{s}^{-1}$ ; b) Versus ageing time A: One week; B: Seven weeks; C: One year

During the crystallizations under illumination, the light intensity was  $5 \text{ mW cm}^{-2}$ .

#### *Variable heating rate and constant wavelength*

Figures 4 and 5 show respectively the qualitative aspect of the DTA curves running under  $\lambda = 546 \text{ nm}$ , for  $0.05$ ,  $0.1$  and  $0.2 \text{ degree s}^{-1}$  heating rates, and their exploitation following the method described before, in reduced coordinates.

It appears that the crystallization occurs mainly through heterogeneous nucleation from initial nuclei, because the slopes 1 and 2 are preponderant. Nevertheless, for the high temperatures just below the top of the crystallization peak, the homogeneous nucleation becomes noticeable (region of slope 4). This is corroborated by the disappearance of the region of slope 2 with the increase of the heating rate, which shifts crystallization peak towards higher temperatures.

#### *Variable wavelength and constant heating rate*

In Figs 6 and 7, we notice the influence of absorption. There is a great difference in the crystallizations between those run under weakly absorbed wavelength and those under strongly absorbed ( $404 \text{ nm}$ ).

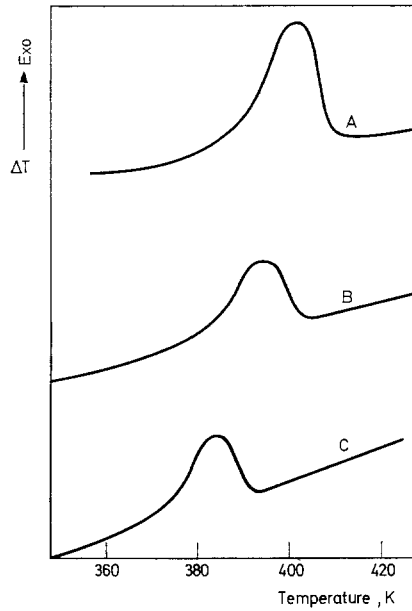


Fig. 4. Exothermic peaks of crystallization versus heating rate (under illumination at 546 nm).  
 A: 0.2 degree · s<sup>-1</sup>; B: 0.1 degree · s<sup>-1</sup>; C: 0.05 degree · s<sup>-1</sup>

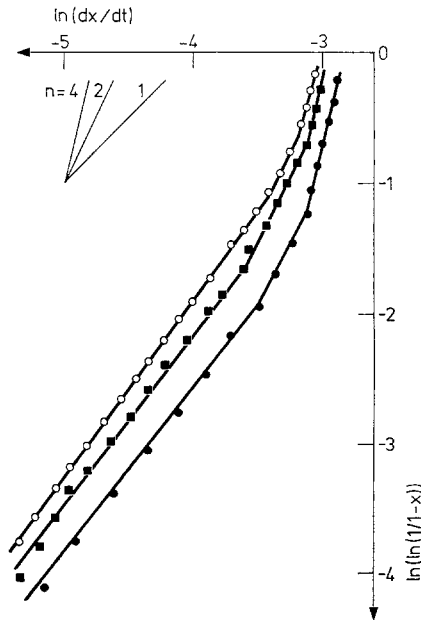


Fig. 5. Experimental exploitation in reduced coordinates (under illumination at 546 nm).  
 Heating rate = ○ — 0.2 degree · s<sup>-1</sup>; ■ — 0.1; ● — 0.05

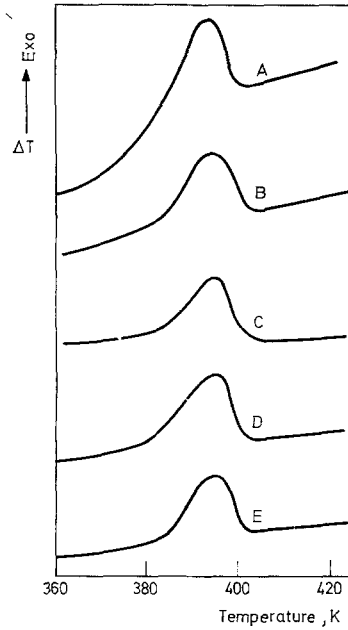


Fig. 6. Exothermic peaks of crystallization (at constant heating rate 0.1 degree s<sup>-1</sup>) vs. wavelength of illumination. A λ = 404 nm; B λ = 546 nm; C λ = 581 nm; D λ = 643 nm; E in the dark

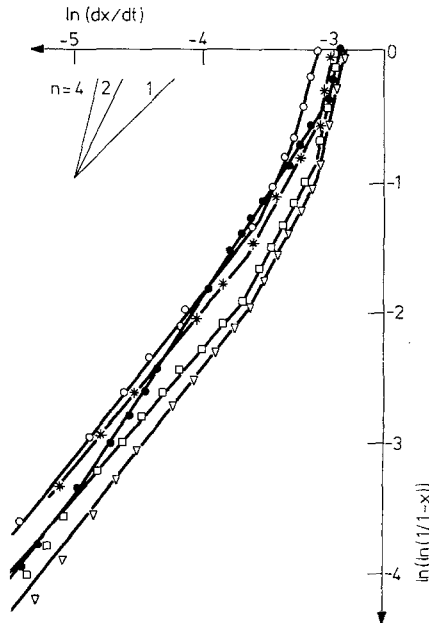


Fig. 7. Experimental exploitation in reduced coordinates (at constant heating rate 0.1 degree s<sup>-1</sup>). ○ λ = 643 nm; \* λ = 581 nm; □ λ = 546 nm; ▽ in the dark; ● λ = 404 nm

### Crystallization parameters [4, 5, 13, 15]

#### *Determination of a growth rate*

For isothermal annealing, the growth rate  $v$  is given by

$$v = v_0 \exp\left(-\frac{E}{kT}\right) \left[1 - \exp\left(-\frac{\Delta G_v}{kT}\right)\right] \quad (15)$$

where  $E$  is the activation energy for one atom to leave the amorphous phase to cross the interface and be fixed to the crystallite and  $\Delta G_v$ , the change in free energy per mole.

When  $T$  (crystallization of amorphous-Se) is far below  $T_m$  (melting point),  $\exp\left(-\frac{\Delta G_v}{RT}\right)$  is very small compared to 1, and the growth rate obeys an Arrhenius equation:

$$v = v_0 \exp\left(-\frac{E}{kT}\right). \quad (16)$$

For this reason, it is impossible to determine the growth rate by the method described before. This method is suitable only if the transformation is an isothermal one.

Thus, for a non-isothermal crystallization, we have to determine an isothermal regime at a temperature  $T_e$ , we call "equivalent temperature", for which, to a good approximation, the crystallization is equivalent to the non-isothermal one (this method is described in appendix A5).

The Table 1 collects different results of  $v$  vs.  $T_e$  and  $\lambda$ . The activation energy  $E$  of  $v$  does not depend on the wavelength. On the other hand, the pre-exponential factor depends on light absorption (Fig. 8). The mean value of  $E$  is 0.70 eV.

#### *Determination of $a_0$ and $p$*

The curves in reduced coordinates as those of Figs 5 and 7 show a change of crystallization regime: first  $n = 1$  and then  $n = 2$ . Following Eq. (11), the  $\ln(1-x)^{-1}$  behavior is at first  $\lambda_1 t$  for  $t < \tau$ , and next  $\lambda_2 t^2$  (for  $t > \tau$ ).

The Eq. (10b) gives:

$$\ln(1-x)^{-1} = p\pi(a_0 + vt)^2.$$

Then, when  $a_0$  is higher than  $vt$  (for the small values of  $t$ ), the principal term is  $2p\pi a_0 vt$  and alternatively (high values of  $t$ ) the term  $p\pi v^2 t^2$  becomes preponderant. Then

$$p = \frac{\lambda_2}{\pi v^2} \quad (17a)$$

and

$$a_0 = \frac{\lambda_1}{2p\pi v} = \frac{\lambda_1}{2\lambda_2} v. \quad (17b)$$

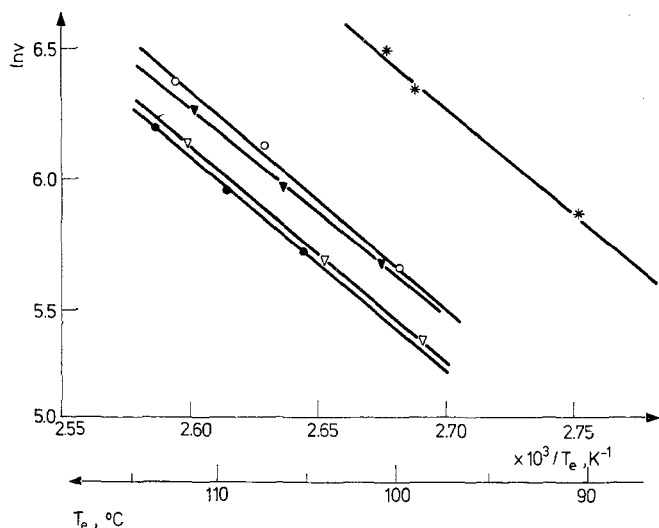


Fig. 8. Arrhenius plot of the growth rate. ★  $\lambda = 404$  nm; ○  $\lambda = 546$  nm; ▼  $\lambda = 581$  nm; ▽  $\lambda = 643$  nm; ● in the dark

The plots of  $\ln(1 - x)^{-1}$  vs.  $t$  (if  $n = 1$ ) and  $t^2$  (if  $n = 2$ ) give respectively the slopes  $\lambda_1$  and  $\lambda_2$ . As the regime is a non-isothermal one, these curves are not straight lines, so  $\lambda_1$  is determined at time  $t_e$  corresponding to equivalent temperature  $T_e$ , and  $\lambda_2$  at the change of regime (Fig. 9).

Table 1

$\lambda_{nm}$	Heating rate, degree · s <sup>-1</sup>	0.05	0.1	0.2
Darkness	$T_e$ , K	378	382.4	386.5
	$v$ , Å s <sup>-1</sup>	306.8	389	492.8
643	$T_e$	371.6	377	384.8
	$V$	217.2	295.5	461.9
581	$T_e$	373.8	379.4	384.4
	$V$	295.5	388.2	526.3
546	$T_e$	373	380.4	385.3
	$V$	283.6	460.9	582
404	$T_e$	363.1	372.2	373.5
	$V$	351.1	567.3	651

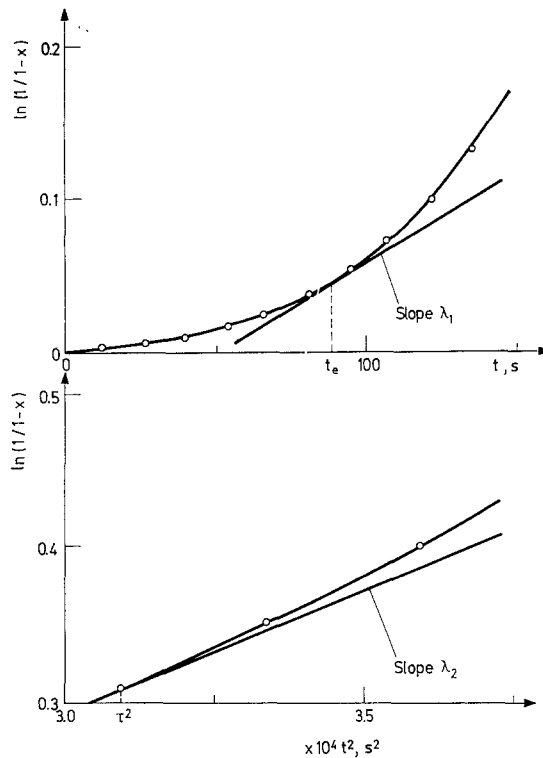


Fig. 9. Up: variation of  $\ln\left(\frac{1}{1-x}\right)$  vs.  $t$  the slope  $\lambda_1$  is calculated at time  $t_e$ . Down: variation of  $\ln\left(\frac{1}{1-x}\right)$  vs.  $t^2$  the slope  $\lambda_2$  is calculated at  $\tau^2$

Table 2 gives the different values of  $a_0$  and  $p$  obtained vs. heating rate  $r$  and  $\lambda$ . This method permits only an estimation of  $a_0$  and  $p$ . It appears that these entities are not affected by  $r$  or  $\lambda$ , but depend on conditions of preparation [16–22].

#### Determination of nucleation rate $N$

All the figures in reduced coordinates show a 4-type region, corresponding to a bulk homogeneous nucleation. This one occurs later in the non-isothermal crystallization (in fact it is hidden for quite a long time by the heterogenous crystallization induced by initial nuclei). According to Eqs (7a) and (11), in an isothermal crystallization  $N$  can be determined by

$$N = \frac{3 \lambda_4}{\pi v^3} \quad (18)$$

where  $\lambda_4$  is the slope of  $\ln(1-x)^{-1}$  plotted vs.  $t^4$ . This is a non-isothermal crystallization and the growth rate depending on temperature has not the same value in

Table 2

$\lambda_{nm}$	Heating rate, degree · s <sup>-1</sup>	0.05		0.1		0.2	
		$a_0$ , m	$p$ , m <sup>-2</sup>	$a_0$	$p$	$a_0$	$p$
Darkness	$a_0$ , m	1.2	10 <sup>-6</sup>	0.82	10 <sup>-6</sup>	0.61	10 <sup>-6</sup>
	$p$ , m <sup>-2</sup>	3.24	10 <sup>9</sup>	4.63	10 <sup>9</sup>	6.23	10 <sup>9</sup>
643	$a_0$	0.77	10 <sup>-6</sup>	1.09	10 <sup>-6</sup>	0.70	10 <sup>-6</sup>
	$p$	6.75	10 <sup>9</sup>	5.88	10 <sup>9</sup>	1.07	10 <sup>10</sup>
581	$a_0$	1.18	10 <sup>-6</sup>	1.03	10 <sup>-6</sup>	0.96	10 <sup>-6</sup>
	$p$	3.45	10 <sup>9</sup>	4.33	10 <sup>9</sup>	5.6	10 <sup>9</sup>
546	$a_0$	1.12	10 <sup>-6</sup>	1.17	10 <sup>-6</sup>	1.02	10 <sup>-6</sup>
	$p$	3.83	10 <sup>9</sup>	3.41	10 <sup>9</sup>	0.96	10 <sup>9</sup>
404	$a_0$	0.93	10 <sup>-6</sup>	1.39	10 <sup>-6</sup>	1.01	10 <sup>-6</sup>
	$p$	2.18	10 <sup>9</sup>	0.95	10 <sup>9</sup>	1.37	10 <sup>9</sup>

the 4-region as in the equivalent isothermal regime in 1-region. In the same way  $N$  depends on temperature, but for a given DTA curve, the temperature range of the 4-region is small enough (within 3 degrees) to consider, as a first approximation, that  $N$  is constant.

If this assumption is correct, the plot of  $\ln(\ln(1-x)^{-1})$  versus  $T^{-1}$  in the 4-type region, for a given DTA curve, has also a linear behavior, with a slope  $-\Delta H/k$  equal to  $-3E/k$ . On the Fig. 10 we have plotted  $\ln(\ln(1-x)^{-1})$  versus  $T^{-1}$  for two scans running at 0.2 degree s<sup>-1</sup> under illumination (404 nm) and in the dark. The two curves have the same slope and we can deduce the common apparent activation energy  $\Delta H$  equal to 2.33 eV. This value is nearly close to  $3E$  (2.1 eV). The slight difference justifies the validity of the proposed assumption.

Taking into account these remarks, we can determine  $N$  (see appendix A6) by:

$$N = \frac{3}{\pi} \frac{1}{v^3} \frac{\lambda_4}{\left[ 4 \exp \left( -\frac{3E(\sqrt{T_p} - \sqrt{T_0})}{2kT_p\sqrt{T_0}} \right) - 3 \right]} \tag{19}$$

where, for a given DTA curve,  $T_p$  is the temperature at the maximum of the crystallization peak,  $T_0$  the temperature of the beginning of 4-region,  $v$  the growth rate at temperature  $T_p$ ,  $\lambda_4$  the slope of the  $\ln(1-x)^{-1}$  plotted versus  $t^4$  determined at time  $t_p$ .

Table 3 collects the obtained data.

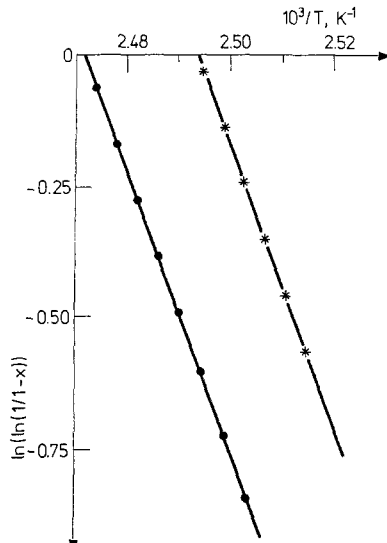


Fig. 10. Variation of  $\ln\left(\ln\left(\frac{1}{1-x}\right)\right)$  vs.  $1000/T$  in the  $n = 4$  region ● in the dark ✱ under illumination at 404 nm

Table 3

$\lambda$ , nm	Heating rate, degree $\cdot$ s $^{-1}$	0.05	0.1	0.2
In the dark	$T_p$ , K	388.2	396	405.6
	$N_m^{-3s-1}$	2.013 $10^{12}$	3.065 $10^{12}$	5.58 $10^{12}$
643	$T_p$	384.2	394.4	400.9
	$N$	2.097 $10^{12}$	2.647 $10^{12}$	5 $10^{12}$
581	$T_p$	384.2	392.7	402
	$N$	1.34 $10^{12}$	2.068 $10^{12}$	4.058 $10^{12}$
546	$T_p$	382.8	392.6	400.6
	$N$	1.73 $10^{12}$	2.52 $10^{12}$	4.48 $10^{12}$
404	$T_p$	381	390.7	398.9
	$N$	3.36 $10^{10}$	1.23 $10^{11}$	1.79 $10^{11}$



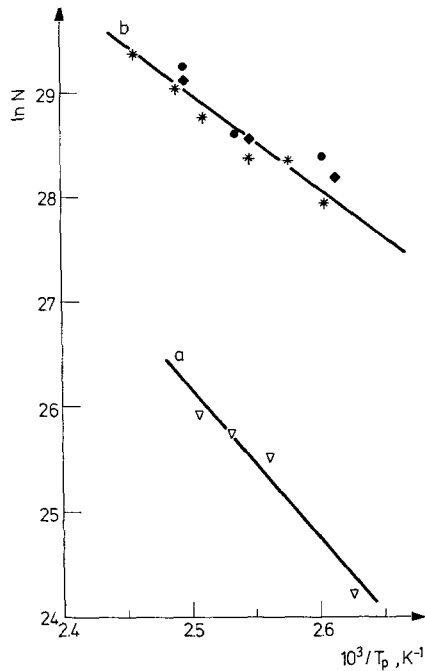


Fig. 11. Arrhenius plot of the nucleation rate per unit volume curve *a*:  $\nabla$   $\lambda = 404$  nm  
 curve *b*:  $\blacklozenge$   $\lambda = 546$  nm;  $*$   $\lambda = 581$  nm;  $\bullet$   $\lambda = 643$  nm;  $*$  in the dark

Figure 11 shows the temperature dependence of  $N$ . An activation energy of 0.8 eV appears for the non or weakly absorbed wavelengths whereas this activation energy is about 1.20 eV under 404 nm illumination. One must take into account these energies in the determination of  $N$ . As we do not, this method can give only approximate values. Corrections are possible on the approximate values of  $N$  by equation (32A); but the general results are not considerably altered by these corrections.

### Conclusion

Usually, the interpretation of DTA or DSC data from the Avrami equation or the Kissinger method is limited to the determination of  $\Delta H$  and  $n$ .

The use of a variable index  $n$  in the Avrami transformation rate equation permits the detection of different types of crystallization. In order to determine the different parameters of the crystallization we have developed an adaptation of an isothermal theory to non-isothermal measurements.

The use of these methods for the crystallization of amorphous-Se films, deposited on Al substrate, in darkness and under illumination shows a predominantly heterogeneous crystallization [21, 22] induced in bulk from the initial nucleation sites.

The density and the mean radius of initial nuclei depends only on sample preparation. The activation energy (0.7 eV) of the growth rate is in good agreement with previous values [16–20]: This energy does not depend on the wavelength of illumination whereas the stronger the absorption factor, the higher the preexponential factor.

We notice a small amount of homogeneous nucleation. In this case, the estimation of the temperature dependence of the nucleation rate shows two different values of the activation energy, 0.8 eV for the weakly absorbed wavelength and 1.2 eV in the opposite case.

## Appendix

### A.1. Relation between $x(t)$ and $\theta$

It has been shown that (Eq. 14):

$$\frac{dx}{dt} = nK_0^{\frac{1}{n}} (1-x) \left[ \ln \left( \frac{1}{1-x} \right) \right]^{\frac{n-1}{n}} \quad (1.A)$$

The temperature dependence of  $K$  is

$$K = K_0 \exp \left( -\frac{\Delta H}{k\theta} \right). \quad (2.A)$$

Since  $r = dT/dt = d\theta/dt$  is constant, equation (1.A) can be integrated

$$\int_0^x \frac{dx'}{(1-x') \left[ \ln(1-x')^{-1} \right]^{\frac{n-1}{n}}} = nK_0^{\frac{1}{n}} \int_0^\theta \exp \left( -\frac{\Delta H}{nk\theta'} \right) \frac{d\theta'}{r}. \quad (3.A)$$

Integration yields

$$\left[ \ln \left( \frac{1}{1-x} \right) \right]^{\frac{1}{n}} = K_0^{\frac{1}{n}} \frac{\theta}{r} E_2 \left( \frac{\Delta H}{nk\theta} \right) \quad (4.A)$$

where  $E_2(y)$  is the exponential integral function of order 2 defined by

$$E_2(y) = \int_1^\infty e^{-yt} \frac{dt}{t^2}. \quad (5.A)$$

### A.2. Determination of $\Delta H/n$ using a single scan

The logarithm of Eq. (1.A) gives

$$\ln \frac{dx}{dt} = -\frac{\Delta H}{nk\theta} + \ln(nK_0^{\frac{1}{n}}) + \ln \left[ (1-x) \left[ \ln \left( \frac{1}{1-x} \right) \right]^{\frac{n-1}{n}} \right]. \quad (6.A)$$

The slope of a plot of  $\ln(dx/dt)$  versus  $\theta^{-1}$  (taking into account that  $x$  is implicitly a function of  $\theta$ ) is  $-\Delta H/nk$ .

A.3. Determination of  $\Delta H$  and  $n$  using a single scan

Note that  $E_2(y)$  can be written

$$E_2(y) = \frac{\exp(-y)}{y + 2} (1 + R(y)) \tag{7.A}$$

where  $R(y) = \frac{2}{(y + 2)^2} +$  higher terms in  $\frac{1}{(y + 2)^2}$  and that in our case  $R$  can be neglected compared to 1; then Eq. (4.A) yields

$$\ln(1 - x)^{-1} = K_0 \left(\frac{\theta}{r}\right)^n \exp\left(\frac{-\Delta H}{k\theta}\right) / \left[\frac{\Delta H}{nk\theta} + 2\right]^n \tag{8.A}$$

and the slope of a plot of  $\ln(\ln(1 - x)^{-1})$  versus  $\theta^{-1}$  is  $-\Delta H/k$ .

A.4.  $n$  can be variable

We can suppose, for instance, that  $n$  takes the  $n_1$  value from  $x = 0$  to  $x = x_1$  and  $n_2$  from  $x = x_1$  to  $x = x_2$ , respectively,  $\theta$  from 0 to  $\theta_1$  and from  $\theta_1$  to  $\theta_2$ . The integration of Eq. (1.A) yields.

$$\begin{aligned} \int_0^{x_1} \frac{dx'}{(1 - x') [\ln(1 - x')^{-1}]^{\frac{n_1 - 1}{n_1}}} + \int_{x_1}^{x_2} \frac{dx'}{(1 - x') [\ln(1 - x')^{-1}]^{\frac{n_2 - 1}{n_2}}} = \\ = n_1 K_0^{\frac{1}{n_1}} \int_0^{\theta_1} \exp\left(-\frac{\Delta H}{n_1 k \theta'}\right) d\theta' + \\ + n_2 K_0^{\frac{1}{n_2}} \int_{\theta_1}^{\theta_2} \exp\left(-\frac{\Delta H}{n_2 k \theta'}\right) d\theta'. \end{aligned} \tag{9.A}$$

Integration gives  
for the left member

$$[\ln(1 - x_2)^{-1}]^{\frac{1}{n_2}} - [\ln(1 - x_1)^{-1}]^{\frac{1}{n_2}} + [\ln(1 - x_1)^{-1}]^{\frac{1}{n_1}}$$

and for the right member

$$K_0^{\frac{1}{n_2}} \frac{\theta_2}{r} E_2\left(\frac{\Delta H}{n_2 k \theta_2}\right) - K_0^{\frac{1}{n_2}} \frac{\theta_1}{r} E_2\left(\frac{\Delta H}{n_2 k \theta_1}\right) + K_0^{\frac{1}{n_1}} \frac{\theta_1}{r} E_2\left(\frac{\Delta H}{n_1 k \theta_1}\right)$$

but

$$[\ln(1 - x_1)^{-1}]^{\frac{1}{n_1}} = K_0^{\frac{1}{n_1}} \frac{\theta_1}{r} E_2 \left( \frac{\Delta H}{n_1 k \theta_1} \right)$$

and

$$[\ln(1 - x_1)^{-1}]^{\frac{1}{n_2}} = K_0^{\frac{1}{n_2}} \frac{\theta_1}{r} E_2 \left( \frac{\Delta H}{n_2 k \theta_1} \right).$$

Therefore

$$\left[ \ln \left( \frac{1}{1 - x_2} \right) \right]^{\frac{1}{n_2}} = K_0^{\frac{1}{n_2}} \frac{\theta_2}{r} E_2 \left( \frac{\Delta H}{n_2 k \theta_2} \right). \quad (10.A)$$

In this equation, the value of  $n$  in the first region does not interfere. Thus, Eq. (4.A) can be valid in different regions where  $n$  can take different values.

#### A.5. Determination of an equivalent isothermal regime and a growth rate

We assume that

$$v = v_0 \exp \left( - \frac{E}{kT} \right). \quad (11.A)$$

a) During an isothermal crystallization  $T$  is a constant and therefore  $v$ . Thus a crystallite growing in the direction perpendicular to the surface, will reach the thickness  $e$  after a time  $\tau$ , and:

$$v = e/\tau$$

b) In a non-isothermal crystallization at the constant heating rate  $r$ , we have to take into account the variation of  $v$  with respect to time.

Let  $x$  be the thickness reached at time  $t$  and  $T_0$  the temperature at the beginning of crystallisation ( $t = 0$ ) and  $T_e$  the temperature when the thickness  $e$  is reached.

$$\frac{dx}{dt} = \frac{dx}{dT} \frac{dT}{dt} = v_0 \exp \left( - \frac{E}{kT} \right) \quad (12.A)$$

$$\frac{re}{v_0} = \int_{T_0}^{T_e} \exp \left( - \frac{E}{kT} \right) dT \quad (13.A)$$

$$\frac{re}{v_0} = T_e E_2 \left( \frac{E}{kT_e} \right) - T_0 E_2 \left( \frac{E}{kT_0} \right) \quad (14.A)$$

$$\frac{re}{v_0} = \frac{E}{k} \left| \frac{E_2(y_e)}{y_e} - \frac{E_2(y_0)}{y_0} \right| \quad (15.A)$$

where  $y = E/kT$

$$\frac{kre}{Ev_0} = f(y_e) - f(y_0) \quad (16.A)$$

where  $f(y) = E_2(y)/y$

We can approximate Eq. (16.A)

$$f(y_e) - f(y_0) \simeq f'(y_m) \cdot |y_e - y_0| \tag{17.A}$$

where  $y_m$  is a value of  $y$  between  $y_0$  and  $y_e$ .

The derivate of  $f(y)$  with respect to  $y$  is

$$f'(y) = - \exp(-y)/y^2 \tag{18.A}$$

thus

$$\delta f = - \frac{\exp(-y_m)}{y_m^2} (y_e - y_0). \tag{19.A}$$

For the expected cases of interest the best approximation is obtained with  $y_m^2 = y_0 y_e$ , and

$$v(T_m) = v_0 \exp\left(-\frac{E}{kT_m}\right) = \frac{er}{T_e - T_0} \tag{20.A}$$

where

$$T_m = \sqrt{T_0 T_e}$$

the temperature  $T_m$  is called "equivalent temperature" because during an isothermal annealing at  $T_m$ , the thickness  $e$  is reached after the time  $(T_e - T_0)/r$ .

#### A.6. Determination of a nucleation rate

For a nucleus generated at time  $\tau$ , its dimension in a direction at time  $t$  is:

$$1 = v_0 \int_{\tau}^t \exp\left(-\frac{E}{kT}\right) dt \tag{21.A}$$

because of the linear variation of  $T$  with  $t$ :  $T = T_0 + rt$ , where  $T_0$  is the temperature at the beginning of crystallization and  $r$  a constant heating rate

$$1 = \frac{v_0}{r} \int_{T_{\tau}}^T \exp\left(-\frac{E}{kT'}\right) dT' \tag{22.A}$$

$T_{\tau}$  is defined by:  $T_{\tau} = T_0 + r\tau$

Per unit volume, there are  $N$  nuclei which are generated between  $\tau$  and  $\tau + d\tau$ . Thus the crystallization volume occupied at time  $t$ , per unit volume, by nuclei generated between  $\tau$  and  $\tau + d\tau$  is:

$$dV = N\eta \left(\frac{v_0}{r}\right)^3 \left[ \int_{T_{\tau}}^T \exp\left(-\frac{E}{kT'}\right) dT' \right]^3 d\tau \tag{23.A}$$

$\eta$  is a shape factor assuming isotropic growing rate, and

$$V(t) = \int_0^t dV. \tag{24.A}$$

If we assume  $N$  constant during one scan

$$V = N\eta \left(\frac{v_0}{r}\right)^3 \int_0^t \left[ \int_{T_\tau}^T \exp\left(-\frac{E}{kT'}\right) dT' \right]^3 d\tau \quad (25.A)$$

$$V = N\eta \frac{v_0^3}{r^4} \frac{E^3}{k^3} \int_{T_0}^T \left[ f\left(\frac{E}{kT}\right) - f\left(\frac{E}{kT_\tau}\right) \right]^3 dT_\tau$$

where  $f(y) = E_2(y)/y$

Using the approximation given by Eqs (16.A) and (17.A), integration of equation yields for the higher terms in  $T$ .

$$\ln \frac{1}{1-x(t)} = \frac{\eta N}{4} [v(T)]^3 \frac{T^4}{r^4} \left[ 4 \exp\left(-\frac{3E}{2kT} \frac{\sqrt{T}-\sqrt{T_0}}{\sqrt{T_0}}\right) - 3 \right]. \quad (26.A)$$

If the growing is spherical  $\eta = \frac{4\pi}{3}$  and according to the time temperature dependence

$$\ln \frac{1}{1-x(t)} \simeq \frac{\pi}{3} N [v(T)]^3 t^4 \left[ 4 \exp\left(-\frac{3E}{2kT} \frac{\sqrt{T}-\sqrt{T_0}}{\sqrt{T_0}}\right) - 3 \right] = \lambda_4 t^4 \quad (27.A)$$

$$\text{with } \lambda_4 = \frac{\pi}{3} N \cdot [v(T)]^3 \left[ 4 \exp\left(-\frac{3E}{2kT} \frac{\sqrt{T}-\sqrt{T_0}}{\sqrt{T_0}}\right) - 3 \right]. \quad (28.A)$$

(If  $T$  is constant during the crystallization, this  $\lambda_4$  is identical to  $\lambda_4$  obtained from Eq. 17.)

Now, using multiple scans we can determine the  $T$ -dependence of  $N$  (because the temperature regions where  $N$  occurs, are different in different scans).

Values of  $N$  obtained by expression (28.A) are approximate values, but normally we have to consider the dependence of  $N$  with temperature following

$$N = N_0 \exp\left(-\frac{G}{kT}\right). \quad (29.A)$$

If we introduce this dependence law in expression (23.A), integration yields for the higher terms in  $T$

$$\ln \left(\frac{1}{1-x}\right) = \frac{N_0}{4} v_0^3 \frac{T^4}{r^4} \exp\left(-\frac{3E}{2kT}\right) \times \left[ 4 \exp\left(-\frac{3E+2G}{2k\sqrt{T_0}T}\right) - 3 \exp\left(-\frac{3E+2G}{2kT}\right) \right]. \quad (30.A)$$

(If in expression (30.A), we assume that  $N$  is constant and equal to its mean value on interval  $T_0 - T$ , i.e.  $N_0 \exp\left(-\frac{G}{kT}\right) \sim N_0 \exp\left(-\frac{G}{k\sqrt{TT_0}}\right)$  expression 30.A leads to expression (27.A).)

We can develop (30.A) in order to obtain  $N(T)$  and in the same way:

$$N(T) = \frac{3 \lambda_4}{\pi [v(T)]^3 \left[ 4 \exp\left(-\frac{3E + 2G \frac{\sqrt{T} - \sqrt{T_0}}{\sqrt{T_0}}}{2kT}\right) - 3 \right]}. \quad (31.A)$$

From the approximate values obtained by (28.A) and an approximate activation energy determined by this way, we can correct these values by:

$$\frac{N(T)}{N_{\text{app}}(T)} = \frac{4 \exp\left(-\frac{3E}{kT} \frac{\sqrt{T} - \sqrt{T_0}}{\sqrt{T_0}}\right) \exp\left(-\frac{G}{kT_0} \frac{\sqrt{T} - \sqrt{T_0}}{\sqrt{T}}\right) - 3}{4 \exp\left(-\frac{3E}{kT} \frac{\sqrt{T} - \sqrt{T_0}}{\sqrt{T_0}}\right) \exp\left(-\frac{G}{kT} \frac{\sqrt{T} - \sqrt{T_0}}{\sqrt{T_0}}\right) - 3} \quad (32.A)$$

In this expression we assume that the approached value  $N_{\text{app}}(T)$  is the  $N$  value at the mean temperature  $\sqrt{TT_0}$ .

## References

1. M. AVRAMI, J. Phys. Chem., 7 (1939) 1103.
2. M. AVRAMI, J. Phys. Chem., 8 (1940) 212.
3. M. AVRAMI, J. Phys. Chem., 9 (1941) 177.
4. P. GERMAIN, K. ZELLAMA, S. SQUELARD and J. C. BOURGOIN, J. Appl. Phys., 50 (1979) 6986.
5. K. ZELLAMA, P. GERMAIN, S. SQUELARD and J. C. BOURGOIN, J. Appl. Phys., 50 (1979) 6995.
6. D. W. HENDERSON, J. Non-Crystal. Sol., 30 (1979) 301.
7. J. W. CAHN, Acta Met., 4 (1956) 449.
8. J. W. CAHN, Acta Met., 4 (1956) 573.
9. H. J. BORCHARD and F. DANIELS, J. Am. Chem. Soc., 79 (1957) 41.
10. H. J. BORCHARD, J. Inorg. Nucl. Chem., 12 (1960) 252.
11. F. O. PILOYAN, I. O. RYABCHIKOV and O. S. NOVIKOVA, Nature, London, 5067 (1966) 1229.
12. H. E. KISSINGER, J. Res. Nat. Bur. Std., 57 (1956) 217.
13. U. KOSTER, Adv. Colloid. Interface Sci., 10 (1979) 129.
14. J. GRENET, J. P. LARMAGNAC and P. MICHON, Thin Sol. Films, 67 (1980) L17.
15. J. W. CHRISTIAN, Theory of transformation in Metals and Alloys 2nd ed., Pergamon, Oxford, 1975.
16. G. FLEURY, A. HAMOU, C. VIGER and C. VAUTIER, Phys. Status Solidi, (a) 64 (1981) 311.
17. K. S. KIM and D. TURNBULL, J. Appl. Phys., 44 (1973) 5237.
18. K. S. KIM and D. TURNBULL, J. Appl. Phys., 45 (1974) 3447.
19. G. GROSS, R. B. STEPHENS and D. TURNBULL, J. Appl. Phys., 48 (1977) 1139.

20. J. DRESNER and G. B. STRINGFELLOW, *J. Phys. Chem. Sol.*, 29 (1968) 303.  
21. J. C. CARBALLE, R. CLEMENT and B. DE CREMOUX, *Rev. Tech. Thomson-CSF*, 5 (1973) 225  
22. D. D. THORNBURG, *Thin Sol. Films*, 37 (1976) 215.

**ZUSAMMENFASSUNG** — Die übliche Bestimmung kinetischer Parameter der Kristallisation amorpher Produkte basiert auf isothermen Messungen. Die Kristallisation von amorphem Selen in dünnen Schichten wird im allgemeinen in nicht-isothermen Experimenten (DTA) untersucht. Die Adaptation der Transformationsgeschwindigkeitsgleichung nach Avrami an die nicht-isotherme Kristallisation ermöglicht die Bestimmung verschiedener Kristallisationstypen. Dadurch wird es möglich, die Veränderungen der Wachstumsgeschwindigkeit und der Geschwindigkeit der Nukleation in Abhängigkeit von der Temperatur zu bestimmen. Der Einfluß der Wellenlänge bei der Bestrahlung während der Kristallisation auf diese Parameter wird ebenfalls untersucht.

**Резюме** — Обычное определение кинетических параметров кристаллизации аморфных продуктов основано на изотермических измерениях. С помощью неізотермического метода (ДТА) изучена кристаллизация тонких аморфных пленок селена. Адаптация к неізотермической кристаллизации уравнения Авраами для скорости превращения, позволило определить различные типы кристаллизации, что в свою очередь дало возможность определить изменение скорости роста и скорости образования центров кристаллизации от температуры. Также исследовано влияние на эти параметры длины волны света, используемого для освещения во время кристаллизации.